Supporting Information

Nanoscale pH-Profile at a Solution/Solid Interface by Chemically Modified Tip-Enhanced Raman Scattering (TERS)

Prompong Pienpinijtham,[a,b,*] Sanpon Vantasin,[a] Yasutaka Kitahama,[a] Sanong Ekgasit,[b] and Yukihiro Ozaki[a,*]

[a]*Department of Chemistry, School of Science and Technology, Kwansei Gakuin University, Sanda, Hyogo 669-1337, Japan.*

[b]*Sensor Research Unit, Department of Chemistry, Faculty of Science, Chulalongkorn University, Pathumwan, Bangkok 10330, Thailand.*

*E-mail: prompong.p@chula.ac.th; ozaki@kwansei.ac.jp.

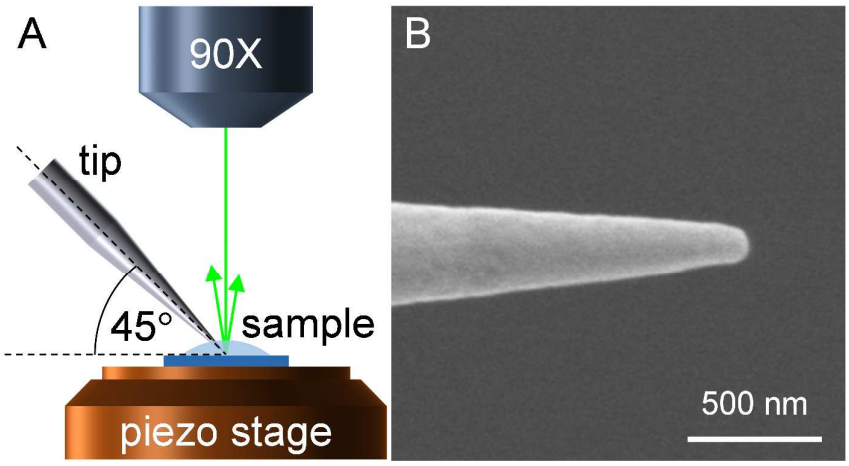

Figure S1. (A) TERS measurement setup used. (B) A SEM image of TERS tip.

Experimental detail

For TERS mapping, after obtaining the AFM image, the piezo stage was retracted 50 nm away from the *p*MBA-modified tip. The distance between the tip and the surface was fixed, so as to (i) eliminate the effect of the distance between the tip and surface on pH measurement, and (ii) avoid damage of the tip from contact with the sample. Remarkably, measuring TERS in a solution can be operated at higher laser power compared to TERS measurement with dry samples because heat accumulation on a tip can transfer to the solution, which reduces largely a degradation of analytes. For measuring TERS spectra in a solution, the feedback system of the piezo stage in the AFM instrument was turned off to prevent auto-rectraction from noncontact mode, and the position of the tip in Z-axis was manually controlled by moving the piezo stage.

_p_MBA-modified TERS tip in different pH solutions

The TERS signals are quite strong due to the direct attachment of the molecules to the tip. Two strong peaks at 1586 and 1079 cm^{-1} are attributed to ring-breathing modes while weak ones at 1422 and 1370 cm^{-1} are attributed to the stretching modes of the carboxylate ($–COO^-$) group. Other small peaks at 1180 and 1138 cm^{-1}, assigned to the C–H bending vibration modes, are also observed (see peak assignments in Table S1). The intensity of the peaks at 1422 and 1370 cm^{-1} increases with an increase in solution pH. This is due to the change in molecular structure of the *p*MBA attached to the tip apex (inset of Figure 1B).[1] The –COOH group is stable in acidic conditions (at low pH). At higher pHs, the –COOH group undergoes OH^--induced proton dissociation to generate $–COO^-$ and H^+. The presence of $–COO^-$ yields peaks at 1422 and 1370 cm^{-1}.

To use the intensity of the peak at 1422 cm^{-1} in Figure 1A for plotting, the peak area in the range of 1460–1360 cm^{-1} was numerically integrated. It is because the spectra are not good enough for peak fitting to consider an individual peak. Moreover, this method also can avoid problems from the peak shift due to the different degree of protonation on the carboxylic groups and the disappearance of peak at 1422 cm^{-1} at pH 7.

Table S1. Peak assignments for *p*MBA and *p*ATP on modified TERS tips.[2-8]

peak frequency (cm^{-1})		
***p*MBA**	***p*ATP**	**assignment**[a,b]
1079		$\nu(CC)_{ring}$
	1079	$\nu(CS)$
1138		$\delta(CH)$
	1145	$\nu(CN)+\delta(CNN)$
1180	1186	$\delta(CH)$
1370		$\nu_{sym}(COO^-)$
	1395	$\delta(CH)+\nu(CC)_{ring}$
1422		$\nu_{asym}(COO^-)$
	1442	$\nu(NN)$
1586	1586	$\nu(CC)_{ring}$

[a] Assignments from refs.[2-8]

[b] δ = bend or deformation; ν = stretch; ring = ring breathing mode; *sym* = symmetric; *asym* = asymmetric.

***p*ATP-modified TERS tip in different pH solutions**

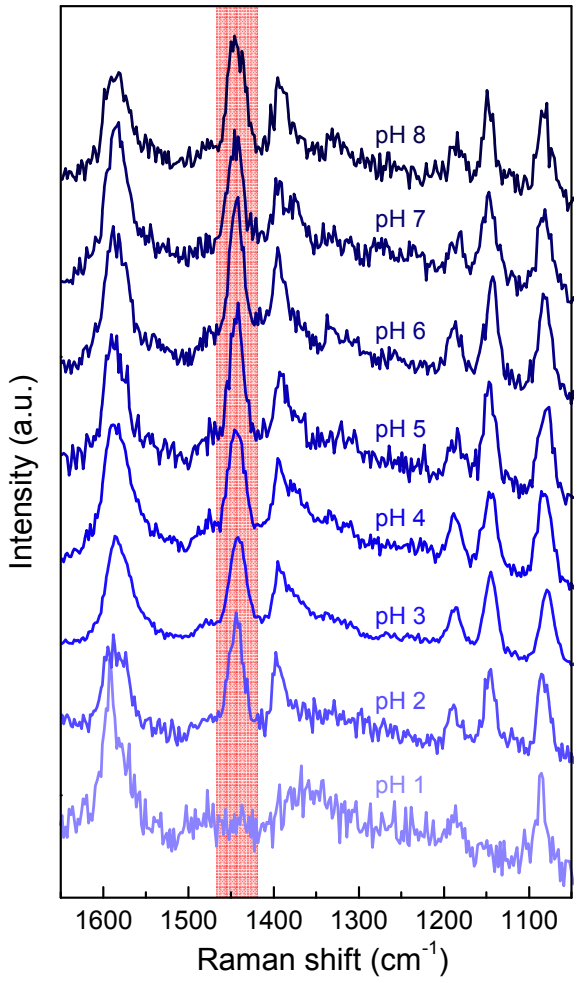

Figure S2. TERS spectra collected from *p*ATP-modified TERS tip in different pH solutions.

A peak at 1586 cm^{-1} is assigned to the CC stretching vibration of the phenyl ring. A peak at 1186 cm^{-1} is attributed to the C–H bending vibration mode, while that at 1079 cm^{-1} is ascribed to the C–S stretching vibration mode. Moreover, there are three strong peaks at 1442, 1395, and 1145 cm^{-1}, which are related to the formation of DMAB. The peak at 1442 cm^{-1} is assigned to the

N=N stretching vibration mode. The peak at 1395 cm^{-1} is a combination of the C–H bending vibration mode and the ring-breathing mode, while that at 1145 cm^{-1} is a combination of the C(in phenyl ring)–N stretching vibration mode and the C–N=N bending vibration mode (see peak assignments in Table S1).

From pH 1–2, these three peaks increase greatly with an increase in pH, indicating that DMAB begins to form in this pH range (see the inset of Figure 2). The peaks at 1442 and 1145 cm^{-1} are more intense because they are directly related to the formation of the N=N moiety. The intensity of the peak at 1395 cm^{-1} increases because the formation of the N=N moiety connects two aromatic rings. A larger π-conjugated system, which possesses higher polarizability, produces a greater increase in the Raman scattering coefficient of the molecule. For higher pH values, these three peaks seem to be slightly more intense, implying that DMAB is slightly more stable at higher pHs. This may be explained by the stabilization of the $–NH_2$ group by H^+. In acidic solutions (at low pH), the $–NH_2$ group is in the form of $–NH_3^+$, preventing two adjacent *p*ATP molecules to form a dimer. On the other hand, at a higher pH, there are more OH^- ions, which promote the deprotonation into $–NH_2$ group. Thus, the formation of DMAB is easily induced.

At lower pH, the noise seems to be poorer than that at higher pH. It is because of the pH-dependent formation of dimer (DMAP), which is a better Raman dye (compared to *p*ATP) due to –N=N– moiety.

Spatial resolution

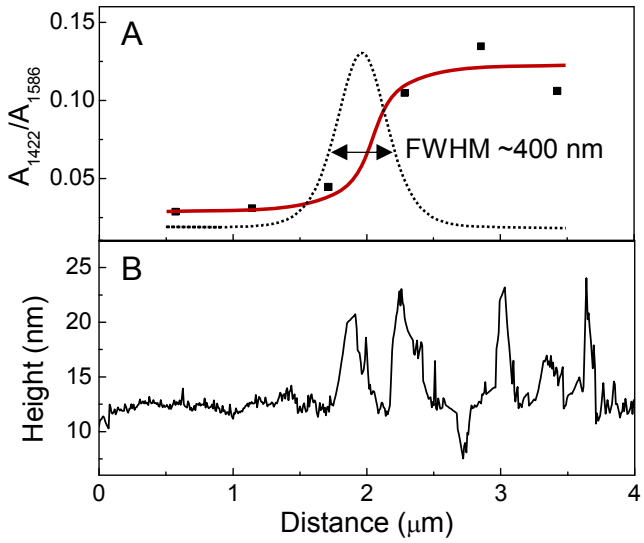

Figure S3. (A) The plot of the ratio of two peaks at 1422 and 1586 cm^{-1} measured from TERS spectra of *p*MBA-modified tip versus distance across the interface between modified and non-modified surfaces of the glass slide. (B) The height of the surface at different positions along the corresponding line in Figure S3A.

To consider the spatial resolution of this measurement, the ratio of two peak areas at 1422 and 1586 cm^{-1}, measured from TERS spectra of the *p*MBA-modified tip, versus distance across the interface between the modified and non-modified surfaces of the glass slide is plotted in Figure S3A. A change in the intensity ratio indicates a change in alkalinity of the surface depending on the modified/non-modified positions, as described above. Figure S3B presents the height of the surface at different positions along the corresponding line in Figure S3A. By comparing Figure S3A and S3B, we can see that the intensity

ratio increases when the height of sample starts to show roughness of surface (at the distance of ~1.8 μm). This is in agreement with the result in Figure 4. By consider the full width at half maximum (FWHM) of derivative (dot line) from the curve used to fit the data points in Figure S3A, the spatial resolution of this method in differentiating modified and non-modified areas is ~400 nm. This is approximately double the distance at which the acidity/alkalinity of the surface can be measured (~200 nm). For the limitation of spatial resolution, it is because the measurements were performed in a solution. The diffusion of OH^- and the induced auto-ionization of water are keys to give poorer spatial resolution compared to dry samples. Moreover, the radius of our TERS tip is approximately 100 nm. To gain better spatial resolution, using smaller TERS tip is one of choices. However, smaller tip may give lower TERS signal.

Raman signal from modified glass slide

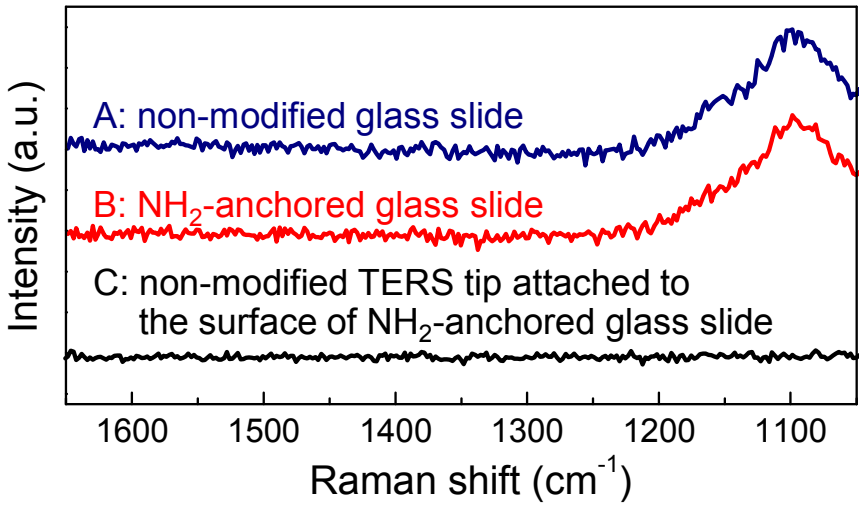

Figure S4. (A) A normal Raman spectrum of a non-modified glass slide. (B) A normal Raman spectrum of an NH_2-anchored glass slide. (C) A TERS spectrum collected from non-modified Ag tip attached to the surface of an NH_2-anchored glass slide.

Normal Raman spectra of a non-modified glass slide and an NH_2-anchored glass slide, together with a TERS spectrum collected from a non-modified Ag tip attached to the surface of the NH_2-anchored glass slide, are displayed in Figure S4. No difference was observed in the normal Raman spectra of the non-modified and modified glass slides by using our setup. There is only a single broad peak at ~1100 cm^{-1}, which is a characteristic peak of SiO_2. Moreover, we could not detect APTMS functionalization on the surface of the modified glass slide using a non-modified Ag tip. From these results, we conclude that using a *p*MBA-modified TERS tip provides useful information

that cannot be obtained from normal Raman scattering or TERS with a non-modified tip.

The deposition of APTMS on a glass slide is not a self-assembled monolayer (SAM). It should be multilayers. A thick tier of silica with amino groups should be formed. A time of 24-hours modification is an intention for making high roughness on a glass slide because the roughness will be employed to indicate a specific location of the modification.[9] Several AFM measurements were scanned around the center regions of glass slide to find the modified/non-modified interface. It is quite difficult to employ other techniques for characterizations of half-modified glass slide because deposited silica tier and glass slide are the same compound, SiO_2. Our normal Raman measurement cannot also observe any change (Figure S4) due to a small amount of hydrocarbon chain and amino groups on a surface. Moreover, using other techniques requires a transfer of sample. Then, the obtained data will not be from the same position with our TERS measurement.

References

1. Talley, C. E.; Jusinski, L.; Hollars, C. W.; Lane, S. M.; Huser, T. Intracellular pH Sensors Based on Surface-Enhanced Raman Scattering. *Anal. Chem.* **2004,** *76*, 7064-7068.
2. Orendorff, C. J.; Gole, A.; Sau, T. K.; Murphy, C. J. Surface-Enhanced Raman Spectroscopy of Self-Assembled Monolayers: Sandwich Architecture and Nanoparticle Shape Dependence. *Anal. Chem.* **2005,** *77*, 3261-3266.
3. Huang, Y.; Dong, B. pH Dependent Plasmon-Driven Surface-Catalysis Reactions of *p*,*p*′-Dimercaptoazobenzene Produced from *Para*-Aminothiophenol and 4-Nitrobenzenethiol. *Sci. China Chem.* **2012,** *55*, 2567-2572.
4. Jiao, L.-s.; Niu, L.; Shen, J.; You, T.; Dong, S.; Ivaska, A. Simple Azo Derivatization on 4-Aminothiophenol/Au Monolayer. *Electrochem. Commun.* **2005,** *7*, 219-222.
5. Michota, A.; Bukowska, J. Surface-Enhanced Raman Scattering (SERS) of 4-Mercaptobenzoic Acid on Silver and Gold Substrates. *J. Raman Spectrosc.* **2003,** *34*, 21-25.
6. Socrates, G. *Infrared and Raman Characteristic Group Frequencies : Tables and Charts*; John Wiley & Sons Inc.: West Sussex, 2008.

7. Kim, K.; Kim, K. L.; Shin, K. S. Photoreduction of 4,4′-Dimercaptoazobenzene on Ag Revealed by Raman Scattering Spectroscopy. *Langmuir* **2013,** *29*, 183-190.

8. Zong, S.; Wang, Z.; Yang, J.; Cui, Y. Intracellular pH Sensing Using *p*-Aminothiophenol Functionalized Gold Nanorods with Low Cytotoxicity. *Anal. Chem.* **2011,** *83*, 4178-4183.

9. Howarter, J. A.; Youngblood, J. P. Optimization of Silica Silanization by 3-Aminopropyltriethoxysilane. *Langmuir* **2006**, *22*, 11142-11147.